Performance dependences on multiplication layer thickness for InP/ InGaAs avalanche photodiodes based on time domain modeling

Yegao Xiao[a], Ishwara Bhat[a], and M. Nurul Abedin[b]
[a]ECSE Dept, Rensselaer Polytechnic Institute, 110 8th Street, Troy, NY 12180
[b]Passive Sensor Systems Branch, MS 468, NASA Langley Research Center, Hampton, VA 23681

ABSTRACT

InP/InGaAs avalanche photodiodes (APDs) are being widely utilized in optical receivers for modern long haul and high bit-rate optical fiber communication systems. The separate absorption, grading, charge, and multiplication (SAGCM) structure is an important design consideration for APDs with high performance characteristics. Time domain modeling techniques have been previously developed to provide better understanding and optimize design issues by saving time and cost for the APD research and development. In this work, performance dependences on multiplication layer thickness have been investigated by time domain modeling. These performance characteristics include breakdown field and breakdown voltage, multiplication gain, excess noise factor, frequency response and bandwidth etc. The simulations are performed versus various multiplication layer thicknesses with certain fixed values for the areal charge sheet density whereas the values for the other structure and material parameters are kept unchanged. The frequency response is obtained from the impulse response by fast Fourier transformation. The modeling results are presented and discussed, and design considerations, especially for high speed operation at 10 Gbit/s, are further analyzed.

Keywords: Avalanche multiplication, avalanche photodiodes, photodetectors, semiconductor device modeling, optoelectronic devices, optical fiber telecommunication

1. INTRODUCTION

InP/InGaAs avalanche photodiodes (APDs) are of great importance for applications in modern long haul and high bit-rate optical telecommunication systems with high sensitivities. In today's commercial market for 2.5 and 10 Gbit/s systems, InP/InGaAs APDs distinguish themselves with superior performance characteristics in comparison with other photodiodes. Especially, the separate absorption, grading, charge, and multiplication (SAGCM)[1-3] structure is one of the most practical APD designs with demonstrated performances such as high internal gain, improved reliability[4,5] and high gain-bandwidth product in excess of 100 GHz[6]. Recently, this basic SAGCM structure has been coupled with a resonant cavity[7-10] to achieve improved performance such as low multiplication noise, high quantum efficiency, maximum unity-gain bandwidth and record-high gain-bandwidth products of 290 GHz[7,8]. Waveguide APDs incorporating SA(G)CM structure have also been developed recently[11,12].

In the mean time, better modeling techniques, especially those for time domain modeling, are also being developed to analyze the device performance characteristics including frequency response and bandwidth, and to predict their designing issues. Many efforts have been devoted to the study of frequency response during the evolution of APD history[13-22], among which a simplified approach for time domain modeling has been reported[22]. This approach[22] considered the statistical characteristics of the avalanche process with dead-space length effect[20,21], and showed good agreement with experiments for the SAGCM InP/InGaAs APDs[22]. More recently, this approach has also been successfully used to model the two-dimensional gain (or responsivity) profiles[23,24] and temperature dependent performance characteristics[25,26].

One of the key design parameters, which affects nearly all the APD performance characteristics, is the thickness of the multiplication region, where the internal gain for APD is generated by impact ionization process. However, the time domain modeling early developed and reported[22-26] has not yet give a detailed modeling of the performance dependences on this key parameter. In this work, performance dependences on multiplication layer thickness have been investigated by time domain modeling. These performance characteristics include breakdown field and breakdown voltage, multiplication gain, excess noise factor, frequency response and bandwidth etc. The modeling results are presented and discussed, and design considerations, especially for high speed operation at 10 Gbit/s, are further analyzed. This paper is organized as

follows. In sections 2 and 3, the time domain modeling approach and the modeling details are described, respectively. In section 4, the results are presented, discussed and analyzed. Finally, a summary is given in section 5.

2. TIME DOMAIN MODELING APPROACH

The details for the time domain modeling approach were presented previously[22-26]. The approach began with the ionization probability coefficients, α for electrons and β for holes, with dead-space effect by taking the avalanche process of carriers as a statistical process. Because of the nonlocalized property of the ionization process, the effect from the dead-space length[20,21], which each carrier has to travel before reaching the ionizing threshold energy, has been incorporated to determine the ionization probability. Then, based on relevant rate equations and analyses of the transit processes of carriers within the depletion region, one can derive the following recurrence relations for carrier density $n(i,j)$ and $p(i,j)$, where i and j denote position and time segment numbers, respectively.

$$n(i,j) = n(i-i_c, j-1) + n1(i-i_c, j-1)[1-\exp(-\alpha i_c \Delta x)] + \sum_{q=0}^{i_c+i_h} p1(i-i_c+q, j-1)\exp\left(-\beta q\frac{i_h}{i_c+i_h}\Delta x\right)\left[1-\exp\left(-\beta\frac{i_h}{i_c+i_h}\Delta x\right)\right] \quad (1)$$

$$p(i,j) = p(i+i_h, j-1) + p1(i+i_h, j-1)[1-\exp(-\beta i_h \Delta x)] + \sum_{q=0}^{i_c+i_h} n1(i+i_h-q, j-1)\exp\left(-\alpha q\frac{i_c}{i_c+i_h}\Delta x\right)\left[1-\exp\left(-\alpha\frac{i_c}{i_c+i_h}\Delta x\right)\right] \quad (2)$$

Here, $n1(x,t)$ and $p1(x,t)$ are denoted as the densities for electrons and holes at position x and time step t which have travelled at least a dead-space distance after generation or last ionizing collision, respectively. In (1) [(2)], the first term on the right is the electron [hole] density at the last position and time segment, the second term denotes the secondary electron [hole] density generated by $n1$ [$p1$], and the third term denotes the secondary electron [hole] density generated by $p1$ [$n1$]. Within one time segment Δt, electrons [holes] travel i_c [i_h] number of position segments Δx with $i_c/i_h = v_{se}/v_{sh}$, where v_{se} and v_{sh} are the absolute values of the saturated velocities for electrons and holes, respectively.

Considering an impulse of incident photon flux at t=0 and with the initial carrier density generated by photon absorption, one can compute the time evolution of carrier density and further obtain the impulse response of photoelectric current density by taking the following averaging procedure,

$$J(j\Delta t) = \frac{\Delta x}{w}\sum_i e\{n(i,j)v_{se}(i) + p(i,j)v_{sh}(i)\} \quad (3)$$

where w is the effective height of the whole active region. Once we have obtained the impulse response density at various bias voltages, fast Fourier transformation (FFT) can be performed to get the response magnitude $|H(f)|$ in the frequency domain.

In order to model the -3 dB bandwidth over a broad range from low to high gain values, additional factors have to be taken into consideration. These factors include the hole trapping at the heterojunction interface between the grading and the absorption layers (see Fig. 1 in next section), the hole diffusion from the undepleted into the depleted absorption region in the low gain (or low bias) range, the gain-bandwidth product limit within the high gain range, and the load circuit (resistance and capacitance product, RC) effect[13,18,22,25,26]. Because these factors affect the -3 dB bandwidth mainly in different gain regimes, as approximations and similar to Ref.[18], we treat them independently. We also assume that the effects of hole trapping and hole diffusion, which are both expected to be very important in the low gain (or low bias) range[27], can be treated separately. However, for simplicity, we neglect the possible effect of hole trapping at the grading layer in this work. The modified frequency response after considering the aforementioned factors can be expressed as follows[25,26],

$$|H'(f)| = \frac{|H(f)|}{\sqrt{1+(2\pi f\tau_{diff})^2}\cdot\sqrt{1+(2\pi fRC)^2}\cdot\sqrt{1+(2\pi f\tau M)^2}} \quad (4)$$

where the three terms in the denominator stand for factors from hole diffusion, *RC* effect and gain-bandwidth product limit, respectively. In (4), τ_{diff} is the hole diffusion time, which can be evaluated by the average thickness of the undepleted absorption region (x_{undep}) and the hole diffusion constant (D_h)[28,29]. Note that when the absorption region is fully depleted, the factor for hole diffusion then becomes unity. Also, for simplicity, we have neglected the effect of hole diffusion when computing the impulse response density in the time domain. The *RC* effect and gain-bandwidth product limit are considered in the same way as in Refs.[18,25,26] In (4), τ is the intrinsic response time through the avalanche multiplication region and τM is the avalanche buildup time. The details on how to calculate τ could be found in Refs.[25,26]

3. MODELING DETAILS

The basic planar SAGCM structure for the In/InGaAs APDs[23-26] is schematically presented in Fig. 1. In Table 1, values for some of the structure parameters, material parameters are listed for the APDs investigated. The other parameter values are similar to those described in Refs.[23-26] The two critical device parameter values, multiplication layer thickness (x_d) and areal charge sheet layer density ($\sigma_{ch}=N_{ch}t_{InP}$) in Table 1, are varied, but with σ_{ch} maintained unchanged when x_d varies. Also, the electric field within the p^+ InP top layer also being taken into consideration. For the performance characteristics within the central active region, the plane junction abrupt approximation can be reasonably used with Fig. 1. Appropriate formulations for determining the electric field profiles $E(x)$ have been set up previously[30].

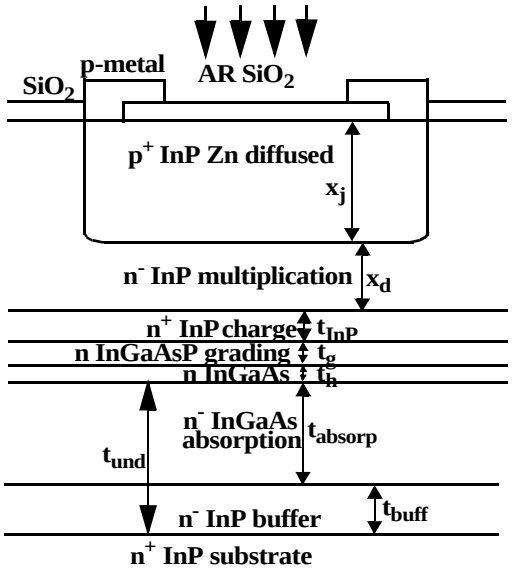

Figure 1: Schematic SAGCM InP/InGaAs APD structure. (For simplicity, details for the guard ring and device periphery are not shown. Note that the figure is not drawn to the scale.)

Table 1. Values for the nominal structure parameters and material parameters used for the SAGCM APDs investigated. (Refer to Fig. 1 for the definitions of the parameters shown.) *x* and *t* are in μm, the doping concentrations *N* are in 10^{15} cm^{-3}, and the areal charge density σ_{ch} is in 10^{12} cm^{-2}. For the Zn diffused p^+ InP layer, a modified diffusion profile from the one in Ref.[30] is used for the modeling. All the parameters listed are at room temperature values.

x_j	2.50	t_{buff}	0
x_d	varying	N_d	0.675
t_{InP}	0.10	σ_{ch}	varying
t_g	0.15	N_g	0.675
t_h	0	N_h	0.675
t_{absorp}	1.0	N_{absorp}	0.3375
t_{sub}	500	N_{sub}	5000
$E_{g\text{-}InP}$	1.35 eV	$E_{g\text{-}InGaAs}$	0.757 eV
$v_{se\text{-}InP}$	80000 m/s	$v_{sh\text{-}InP}$	60000 m/s
C	0.2 pF	R	50 Ω

With the relevant material and modeling parameters determined and the electric field profiles computed, the impulse response density in time domain can be obtained with the aforementioned time domain modeling approach. The value of the multiplication gain (*M*) is determined as the ratio of the area under the time domain impulse response curve with multiplication to that without multiplication, as described in Refs.[22-26] The breakdown voltage is determined as the voltage when the multiplication gain reaches 100. The excess noise factor can be calculated by taking the McIntyre's expression[31] with the ionization coefficients, α and β, generated during the modeling process.

When using (4) to compute the normalized frequency response and to evaluate the -3 dB bandwidth, the total operating capacitance *C* is usually less than 0.3 pF[32] (about 0.20 - 0.23 pF[33,34]), and it is taken as 0.2 pF during our modeling. The

average resistance including load resistance is taken as 50 Ω for our modeling. We also tried to evaluate the intrinsic response time, τ, through the avalanche multiplication region according to the theoretical expression described in Refs.[25,26] But this characteristic parameter depends on several complex factors including the ionization process and multiplication, carrier drift velocity, and particular material and/or device structure etc., the accuracy for the theoretical prediction of this τ value is doubtful in determining the gain-bandwidth product. Nevertheless, the effect of τ*M* on the bandwidth should be qualitatively acceptable for the results presented when varying the multiplication layer thickness.

4. RESULTS ANALYSES AND DISCUSSION

In Fig. 2, the breakdown field profiles are shown with different multiplication layer thicknesses with the areal charge sheet density fixed at 3.1×10^{16} m^{-2}. The breakdown field, the maximum electric field at the interfaces between the top Zn diffused p^+ layer and the n^- InP multiplication layer decreases monotonously as the multiplication layer gets enlarged. This is because, for a wide multiplication layer, carriers can travel longer distance with low electric field to reach the threshold energy at which the impact ionization process can be initiated. For thin multiplication layer, the electric field has to be high enough for the carriers to gain enough energy with small travelling distance. It should also be noted that the electric field profile extends about 0.25 μm into the top Zn diffused p^+ layer. This means that the effective multiplication region may be actually larger than the nominal values listed in Fig. 2.

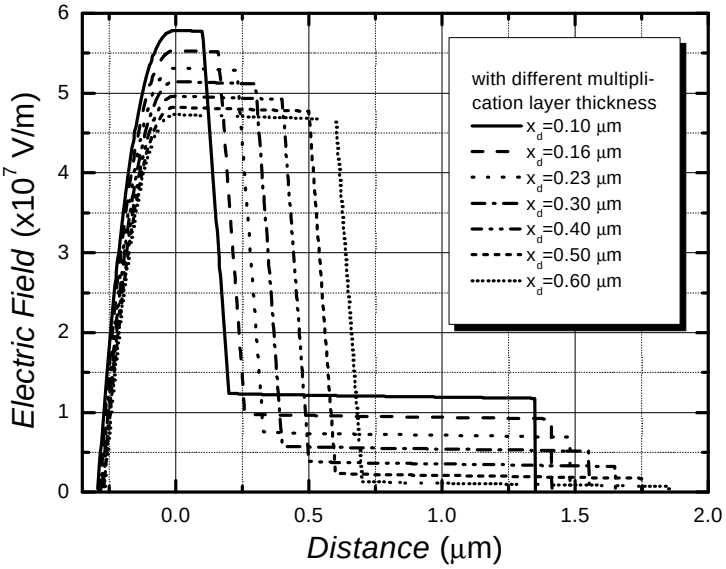

Figure 2: Electrical field profiles at breakdown for different multiplication layer thicknesses. The areal charge sheet layer density is kept unchanged at 3.1×10^{16} m^{-2}.

The curves of multiplication gain versus reverse bias voltage are presented in Fig. 3 with different multiplication layer thicknesses and fixed value of 3.1×10^{16} m^{-2} for areal charge sheet denssity. One characteristic voltage, the punch-through voltage[30], at which the gain increases from unity, corresponds to the voltage at which the InGaAs layer just starts to be depleted. All the InGaAs layers including the transport layer t_h (no such a layer for the actual modeling in this work) function as absorption region for photon incident impulses. The carriers (holes) generated by photon absorption within the depleted absorption region will transit into the multiplication layer to initiate impact ionization and generate multiplication gain. For APDs with thin multiplication layer, the absorption region can be easily depleted with low punch-through voltages. However, for the APDs with large multiplication layer thickness, the heavily doped charge sheet layer makes the electric field drop to zero without depleting the absorption region unless reaching the high punch-through voltages. In order to deplete fully the absorption region for APDs with large multiplication layer, high reverse bias voltage have to be applied to raise the electric field in the multiplication region. But as seen from Fig. 3, the punch-through voltage becomes close to and eventually will merge with the breakdown voltage when the multiplication layer becomes very large. Therefore, those devices with large multiplication layer thickness are actually not practical from the application operation point of view because such devices will have reliability problem when operated in such a close proximity to breakdown.

From Fig. 3, one could obtain the breakdown voltage values with different multiplication layer thicknesses. Such curves are demonstrated in Fig. 4, where breakdown voltages are plotted versus multiplication layer thickness for four areal charge sheet layer density values, $2.9x10^{16}$, $3.1x10^{16}$, $3.3x10^{16}$, and $3.5x10^{16}$ m^{-2} respectively. These curves all show non-monotonous dependence on the multiplication layer thickness, and a minimum is found at about 0.225 μm for the nominal multiplication layer thickness. This feature is qualitatively consistent with the simulation results based on traditional multiplication formula as reported by Itzler et al[33,35] and by Park et al.[36] The explanation for this minimum could be referred to Fig. 2. The breakdown voltage values are high for both thin and wide multiplication regions because in the former situation, the increased electric field can result in large voltage drop outside the multiplication region, and in the latter situation, the large voltage can drop across over the multiplication region. Although the minimum seems unchanged with different areal charge sheet density, the feasible operation bias voltage (as seen by the breakdown voltage) is limited for APDs with wide multiplication layer and high areal charge sheet density due to the aforementioned analyses for Fig. 3.

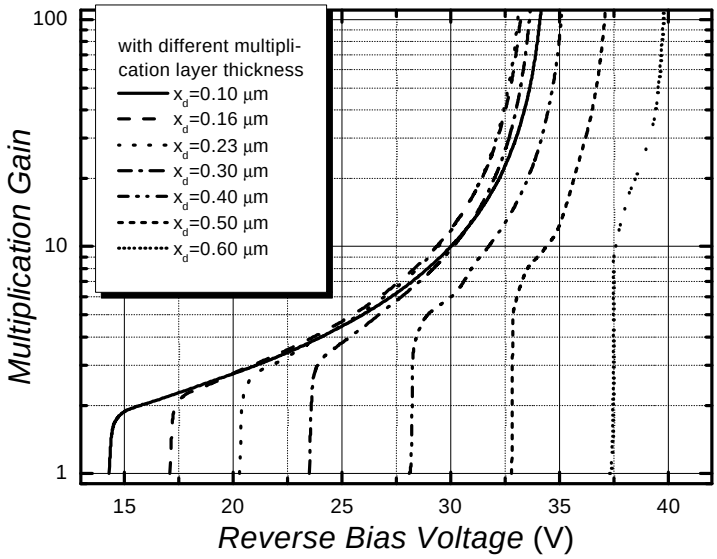

Figure 3: Multiplication gain versus reverse bias voltage for different multiplication layer thicknesses. The areal charge sheet layer density is kept unchanged at $3.1x10^{16}$ m^{-2}.

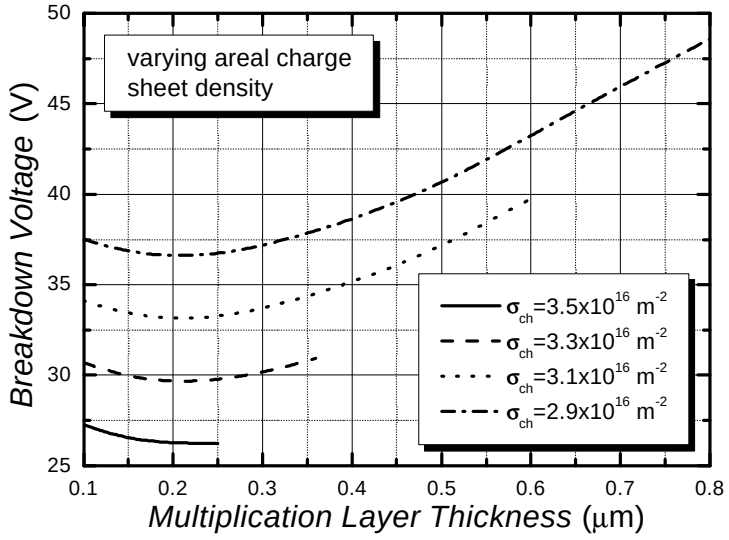

Figure 4: Breakdown voltage versus multiplication layer thickness for four areal charge sheet density values as labeled.

The plottings for excess noise factor versus multiplication gain are presented in Fig. 5 with different multiplication layer thicknesses. For APDs with thinner multiplication layer, the excess noise factor is higher. This corresponds to the higher

electric field for ionization process for thinner multiplication region, which increases the effective ratio of the ionization coefficients (k_{eff}=α/β)[30]. For stable bit-rate response, the APDs operate mostly within an operational bandwidth ceiling gain range up to 12 or maybe up to 16 in some cases, the excess noise factor within this gain range can be taken as in the similar value level for all the multiplication layer thicknesses investigated. Primary concern for the APD performance should be on the bandwidth characteristics with wide bandwidth ceiling gain range.

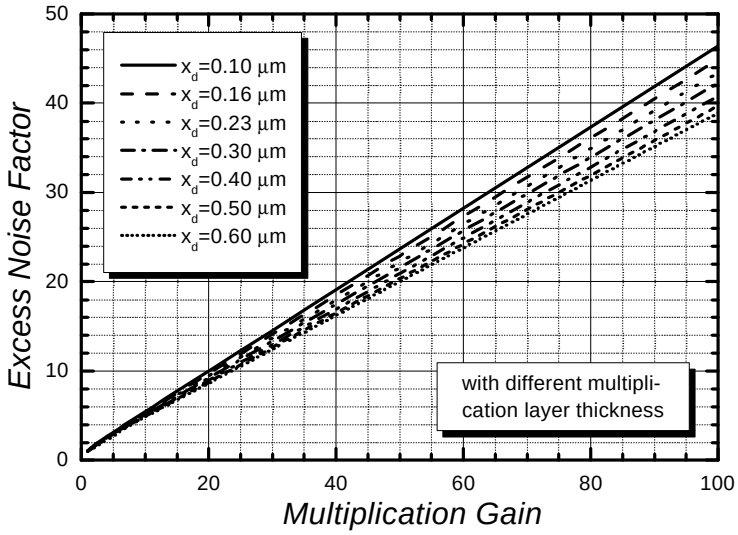

Figure 5: Excess noise factor versus multiplication gain for different multiplication layer thicknesses. The areal charge sheet layer density is kept unchanged at $3.1x10^{16}$ m^{-2}.

The curves for the -3 dB bandwidth versus multiplication gain are presented in Fig. 6 with different multiplication layer thicknesses. An ideal bandwidth characteristics would request that the high bandwidth ceiling could be achieved with as low multiplication gain (M_{lower}) as possible and this high bandwidth ceiling range can extended to as high multiplication gain (M_{upper}) as possible without deteriorating the stable bit-rate operation. As seen in Fig. 6, the device with wide multiplication layer should be avoided due to its low bandwidth value and large M_{lower} value. The poor bandwidth ceiling or even unavailable ceiling range makes this kind of devices not feasible for operation at all. Physically, it is not difficult understand the bandwidth feature for APDs with wide multiplication layer. Firstly, the wide multiplication region means that the carriers have to spend longer time to go through the impact ionization processes before they could be swept to the top p^+ contact terminal for current collection. Secondly, the wide multiplication region also means a high avalanche buildup time which will decrease the bandwidth at high gain value significantly. This will result in low gain-bandwidth product. Apparently, APDs with small multiplication layer should be considered when trying to optimize the device design. This can be also seen in Fig. 7, where the maximum bandwidths for the bandwidth ceiling region and the multiplication gain values for these maximum bandwidths are plotted versus the multiplication layer thicknesses with areal charge sheet density maintained at $3.1x10^{16}$ m^{-2}.

Although the avalanche buildup time evaluated in this work may not be able to give an accurate prediction comparable to the actual devices, qualitatively, it is obvious that the APDs with thin multiplication layer will result in enhanced (or high) gain-bandwidth product as seen by the curves in Fig. 6. The APDs with thin multiplication region are expected to have high maximum bandwidths as seen in Fig. 7 with wide bandwidth ceiling range as seen in Fig. 6. These devices will provide more stable and reliable operation in comparison with those with wide multiplication layers.

Among the three key parameters for an SAGCM APD design, the absorption layer thickness has to be maintained at about 1 μm (or down to 0.8 μm when using microlens) to achieve unity-gain responsivity at 0.7 A/W. So there is no space to reduce further the absorption layer to improve the bandwidth. An optimized design considerations for 10 Gbit/s operation rely mainly on adjusting the multiplication layer thickness by controlling the Zn diffusion depth into the grown n^- InP layer and on adjusting the areal charge sheet p^+ InP layer density appropriately. Taking the approximate "rule-of-thumb"

relationship[37] between the -3 dB bandwidth of the optoelectric current frequency response, BW_{el}, and the maximum transmission bit rate, B, i.e., $\sqrt{2}BW_{el} \cong B$, one could see from Fig. 6 that APDs with multiplication layer thickness less than 0.3 μm should be fine to satisfy this rule with reasonable bandwidth ceiling range above 7.07 GHz. For the multiplication layer from 0.3 μm to 0.4 μm, the APDs may work for some gain range, but the performance is not optimal. By appropriately choosing the areal charge sheet density (both the dopant density and the thickness of the charge sheet layer), APDs with multiplication layer thickness less than 0.3 μm should give good performances for high speed operation at 10 Gbit/s.

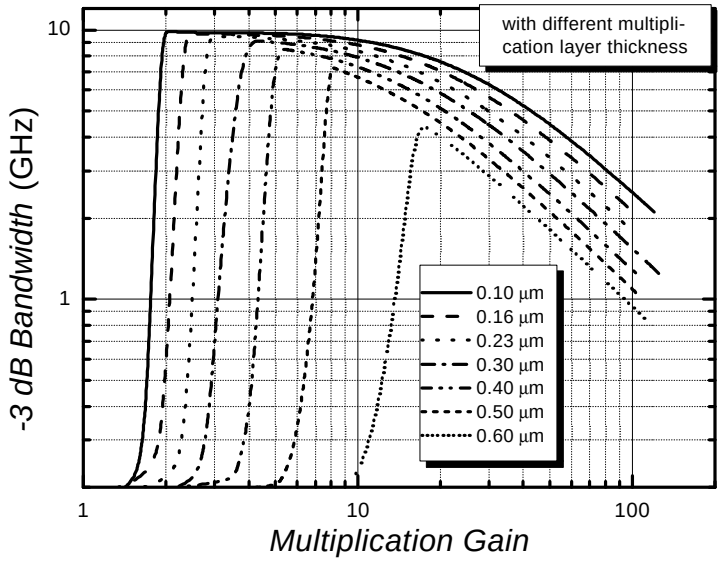

Figure 6: -3 dB bandwidth versus multiplication gain for different multiplication layer thicknesses. The areal charge sheet layer density is kept unchanged at 3.1×10^{16} m^{-2}.

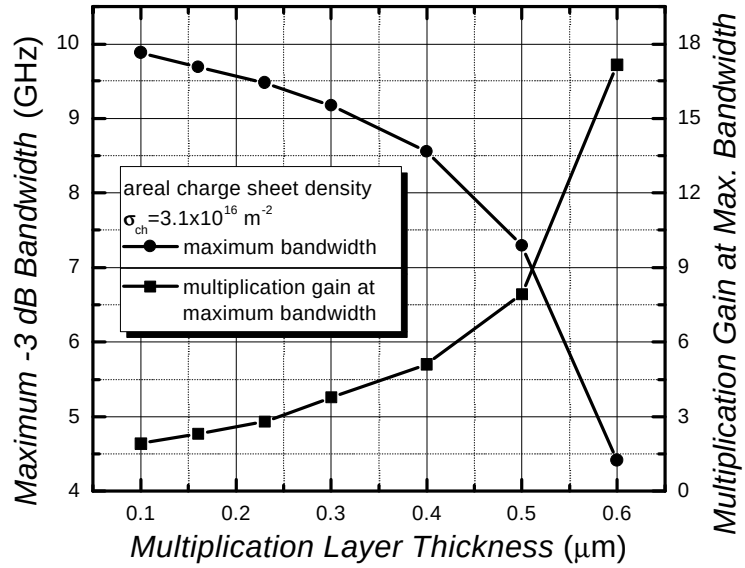

Figure 7: Maximum -3 dB bandwidth versus multiplication layer thickness and multiplication gain at maximum -3 dB bandwidth versus multiplication layer thickness.

Although Fig. 6 also indicates that, by taking the thinnest multiplication layer, the M_{lower} value could be reduced to widen the bandwidth ceiling range, the multiplication layer as thin as 0.1 μm might be technically difficult to achieve because it is controlled by the top Zn diffusion depth. Our early analyses[24] suggests that the top Zn diffusion is a very crucial process step to obtain uniform responsivity profile especially when depressing premature edge breakdown in the device periphery

region has to be taken into consideration. It has also been reported that very thin multiplication layer may lead to premature edge breakdown[35]. The optimal APD design involves several points of trade-off considerations when all the aspects of performance characteristics are evaluated. From the viewpoint of depressing premature edge breakdown and also the technical consideration, very thin multiplication layer is not a feasible choice. As seen from Fig. 4, an appropriate choice of multiplication layer thickness will be near the valley bottom (from 0.2 to 0.3 μm) where breakdown voltage minimum occurs.

By keeping the multiplication layer thickness at 0.16 μm, the bandwidth characteristics versus multiplication gain have also been modeled for different values of areal charge sheet density. Lowering the areal charge sheet density helps to reduce the M_{lower}, but the bandwidth at high gain values seems unaffected. However, low areal charge sheet density will lead to high breakdown voltage (or correspondingly high operating voltage) which will worsen the power consumption issue. Low power consumption is an important issue for a device to maintain stable and reliable operation with reasonably long lifetime. From all these analyses and our modeling results, it can be concluded that an optimal APD design for stable and reliable 10 Gbit/s operation will have 0.2-0.3 μm, $3.1x10^{16}$-$3.3x10^{16}$ m^{-2}, and 1 μm for the three key parameters, multiplication layer thickness, areal charge sheet density and the absorption layer width, respectively.

Before concluding this paper, some points of simplifications for the modeling in this work should be mentioned. For example, hole trapping was neglected and this will affect the accuracy at low multiplication gain region including the bandwidth. The hole diffusion was ignored when computing the impulse response density in the time domain and this might affect the accuracy of the multiplication gain at low bias voltages. A single operating capacitance (0.2 pF) is assumed for all the APDs with different multiplication layer thicknesses and this rough treatment will also affect the accuracy of the bandwidth. As a matter of fact, when the absorption layer is partially depleted, the device capacitance will be also different from that when the device is fully depleted. The avalanche buildup time was evaluated according to the theoretical expressions described in Refs,[25,26] but these theoretical expressions had origin actually from some early developed theories for silicon APDs[38,39]. Their applicability to compound semiconductor APDs needs to be explored, and our results already indicate that the poor accuracy for the bandwidths at high gain region beyond the bandwidth ceiling. Somehow, reasonable values for the gain-bandwidth product could not be obtained. Nevertheless, improvement over these simplifications are expected to be addressed in future work.

5. SUMMARY

Time domain modeling has been conducted to investigate the performance dependences on multiplication layer thickness for InP/InGaAs SAGCM APDs. These performance characteristics include breakdown field and breakdown voltage, multiplication gain, excess noise factor, frequency response and bandwidth etc. The simulations are performed versus various multiplication layer thicknesses with certain fixed values for the charge sheet density whereas the other structure and material parameters are kept unchanged. The modeling results are presented, analyzed and discussed. From our modeling results and analyses, it can be concluded that an optimal APD design for stable and reliable 10 Gbit/s operation will have 0.2-0.3 μm, $3.1x10^{16}$-$3.3x10^{16}$ m^{-2}, and 1 μm for the three key parameters, multiplication layer thickness, areal charge sheet density and the absorption layer width, respectively.

ACKNOWLEDGMENTS

The author, Y. G. Xiao, would like to thank Prof. M. J. Deen for the supervision over Xiao's Ph D thesis on APD modeling. This work was partially supported by NASA Langley Research Center.

REFERENCES

1. L. E. Tarof, D. G. Knight, T. Baird, K. E. Fox, C. J. Miner, N. Puetz, and H. B. Kim, "Planar InP/InGaAs avalanche photodetectors with partial charge sheet in device periphery," Appl. Phys. Lett., **57**, pp. 670-672, 1990.
2. P. P. Webb, R. J. McIntyre, J. Scheibling, and M. Holunga, "Planar InGaAs/InP APD fabrication using vapor-phase epitaxy and silicon implantation techniques," in *Optical Fiber Communications Conf.*, Washington, DC: Optical Society of America, (Technical Digest Series) Vol. **1**, pp. 129-130, 1988.

3. R. Kuchibhotla, and J. C. Campbell, “Delta-doped avalanche photodiodes for high bit-rate lightwave receivers,” J. Lightwave Technol., **9**, pp. 900-905, 1991.
4. S. An, M. J. Deen, A. S. Vetter, W. R. Clark, J. -P. Noel, and F. R. Shepherd, “Effect of mesa overgrowth on low-frequency noise in planar separate absorption, grading, charge, and multiplication avalanche photodiodes,” IEEE J. Quantum Electron., **35**, pp. 1196-1202, 1999.
5. S. An, M. J. Deen, “Low-frequency noise in single growth planar separate absorption, grading, charge, and multiplication avalanche photodiodes,” IEEE Trans. Electron. Dev., **47**, pp. 537-543, 2000.
6. L. E. Tarof, “Planar InP/InGaAs avalanche photodetector with a gain-bandwidth product in excess of 100 GHz,” Electron. Lett., **27**, pp. 34-36, 1991.
7. H. Nie, O. Baklenov, P. Yuan, C. Lenox, B. G. Streetman, and J. C. Campbell, “Quantum-dot resonant-cavity separate absorption, charge, and multiplication avalanche photodiode operating at 1.06 μm,” IEEE Photon. Technol. Lett., **10**, pp. 1009-1011, 1998.
8. C. Lenox, H. Nie, P. Yuan, G. Kinsey, A. L. Homles, Jr., B. G. Streetman, and J. C. Campbell, “Resonant-cavity InGaAs-InAlAs avalanche photodiodes with gain-bandwidth product of 290 GHz,” IEEE Photon. Technol. Lett., **11**, pp. 1162-1164, 1999.
9. Y. G. Xiao and M. J. Deen, “Theoretical approach to frequency response of resonant cavity avalanche photodiodes,” Proc. SPIE, Vol. **4288**, pp. 21-30, 2001.
10. Y. G. Xiao and M. J. Deen, “Frequency response and modeling of resonant-cavity separate absorption, charge and multiplication avalanche photodiodes,” J. Lightwave Technol., **19**, pp. 1010-1022, 2001.
11. G. S. Kinsey, J. C. Campbell, and A. G. Dentai, “Waveguide avalanche photodiode operating at 1.55 μm with a gain-bandwidth product of 320 GHz,” IEEE Photon. Technol. Lett., **13**, pp. 842-844, 2001.
12. J. Wei, F. N. Xia, and S. R. Forrest, “A high-responsivity high-bandwidth asymmetric twin-waveguide coupled InGaAs-InP-InAlAs avalanche photodiode,” IEEE Photon. Technol. Lett., **14**, pp. 1590-1592, 2002.
13. J. C. Campbell, B. C. Johnson, G. J. Qua and, W. T. Tsang, “Frequency response of InP/InGaAsP/InGaAs avalanche photodiodes,” J. Lightwave Technol., **7**, pp. 778-784, 1989.
14. R. B. Emmons, “Avalanche-photodiode frequency response,” J. Appl. Phys., **38**, pp. 3705-3714, 1967.
15. G. Kahraman, B. E. A. Saleh, W. L. Sargeant, and M. C. Teich, “Time and frequency response of avalanche photodiodes with arbitrary structure,” IEEE Trans. Electron. Dev., **39**, pp. 553-560, 1992.
16. T. Shiba, E. Ishimura, K. Takahashi, H. Namizaki, and W. Susaki, “New approach to the frequency response analysis of an InGaAs avalanche photodiode,” J. Lightwave Technol., **6**, pp. 1502-1506, 1988.
17. J. N. Hollenhorst, “Frequency response theory for multilayer photodiodes,” J. Lightwave Technol., **8**, pp. 531-537, 1990.
18. J. C. Campbell, W. S. Holden, G. J. Qua, and A. G. Dentai, “Frequency response of InP/InGaAsP/InGaAs avalanche photodiodes with separate absorption ‘grading’ and multiplication regions,” IEEE J. Quantum Electron., **21**, pp. 1743-1746, 1985.
19. W. S. Wu, A. R. Hawkins, and J. E. Bowers, “Frequency response of avalanche photodetectors with separate absorption and multiplication layers,” J. Lightwave Technol., **14**, pp. 2778-2785, 1996.
20. M. M. Hayat and B. E. A. Saleh, “Statistical properties of the impulse response function of double-carrier multiplication avalanche photodiodes including the effect of dead space,” J. Lightwave Technol., **10**, pp. 1415-1425, 1992.
21. M. M. Hayat, B. E. A. Saleh, and M. C. Teich, “Effect of dead space on gain and noise of double-carrier-multiplication avalanche photodiodes,” IEEE Trans. Electron. Dev., **39**, pp. 546-552, 1992.
22. A. Bandyopadhyay, M. J. Deen, L. E. Tarof, and W. Clark, “A simplified approach to time domain modeling of avalanche photodiodes,” IEEE J. Quantum Electron., **34**, pp. 691-699, 1998.
23. Y. G. Xiao and M. J. Deen, “Two-dimensional gain profiles of InP/InGaAs separate absorption, grading, charge, and multiplication avalanche photodiodes modeled by a simplified stochastic approach,” J. Vac. Sci. Technol. A, **18**, pp. 610-614, 2000.
24. Y. G. Xiao and M. J. Deen, “Modeling of two-dimensional gain profiles for InP-InGaAs avalanche photodiodes with a stochastic approach,” IEEE J. Quantum Electron., **35**, pp. 1853-1862, 1999.
25. Y. G. Xiao and M. J. Deen, “Temperature dependent studies of InP/InGaAs avalanche photodiodes based on time domain modeling,” IEEE Trans. Electron Dev., **48**, pp. 661-670, 2001.
26. Y. G. Xiao and M. J. Deen, “Time domain modeling of InP/InGaAs avalanche photodiodes,” Proc. SPIE, Vol. **4288**, pp. 85-93, 2001.

27. N. R. Das and M. J. Deen, “Low bias performance of avalanche photodetector - a time domain approach,” IEEE J. Quantum Electron., **37**, pp. 69-74, 2001.
28. J. M. Senior, *Optical Fiber Communications, Principles and Practice*, (2nd edition), Prentice Hall, 1992.
29. S. Wang, *Fundamentals of Semiconductor Theory and Device Physics*, Prentice Hall, 1989.
30. C. L. F. Ma, M. J. Deen, and L. E. Tarof, “Characterization and modeling of SAGCM InP/InGaAs avalanche photodiodes for multigigabit optical fiber communications,” Advances in Imaging and Electron Physics, **99**, pp. 65-170, 1998.
31. R. J. McIntyre, “Multiplication noise in uniform avalanche diodes,” IEEE Trans. Electron. Dev., **13**, pp. 164-168, 1966.
32. L. E. Tarof, J. Yu, T. Baird, R. Bruce, and D. G. Knight, “Temperature measurements of separate absorption, grading, charge, and multiplication (SAGCM) InP/InGaAs avalanche photodiodes (APD’s)”, IEEE Photon. Technol. Lett., **5**, pp. 1044-1046, 1993.
33. M. A. Itzler, K. K. Loi, S. McCoy, N. Codd, and N. Komaba, “Manufacturable planar bulk-InP avalanche photodiodes for 10 Gb/s applications,” in *IEEE Lasers & Electro-Optic Society 12th Annual Meeting - LEOS’99*, San Francisco, (Technical Digest Series) Vol. **2**, pp. 748-749, 1999.
34. M. A. Itzler, K. K. Loi, S. McCoy, N. Codd, and N. Komaba, “High-performance, manufacturable avalanche photodiodes for 10 Gb/s optical receivers,” in *Optical Fiber Communication Conference - OFC’2000*, Baltimore, (Technical Digest Series) Vol. **4**, pp. 126-128, 2000.
35. M. A. Itzler, C. S. Wang, S. McCoy, N. Codd, and N. Komoba, “Planar bulk-InP avalanche photodiode design for 2.5 and 10 Gb/s applications,” *ECOC’98*, Madrid, pp. 59-60, 1998.
36. C. -Y. Park, K. -S. Hyun, S. -G. Kang, and H. -M. Kim, “Effect of multiplication layer width on breakdown voltage in InP/InGaAs avalanche photodiode,” Appl. Phys. Lett., **67**, pp. 3789-3791, 1995.
37. J. Gowar, *Optical Communication Systems*, Prentice Hall International (UK) Ltd, 2nd edition, p. 26, 1993.
38. R. Kuvas and C. A. Lee, “Quasistatic approximation for semiconductor avalanches,” J. Appl. Phys., **41**, pp. 1743-1755, 1970.
39. I. M. Naqvi, “Effects of time dependence of multiplication process on avalanche noise,” Solid-State Electron., **16**, pp. 19-28, 1973.